frontiers | Frontiers in Earth Science

TYPE Original Research
PUBLISHED 13 January 2023
DOI 10.3389/feart.2022.1031799

Check for updates

OPEN ACCESS

EDITED BY
Hao Zou,
Chengdu University of Technology, China

REVIEWED BY
Bin Cheng,
China University of Petroleum, Qingdao, China
Zeyang Liu,
Chengdu University of Technology, China

*CORRESPONDENCE
Chenchen Fang,
fangchenchen@petrochina.com.cn

SPECIALTY SECTION
This article was submitted to Economic Geology, a section of the journal Frontiers in Earth Science

RECEIVED 30 August 2022
ACCEPTED 31 October 2022
PUBLISHED 13 January 2023

CITATION
Zhai J, Cao Z, Fang C, Yuan Y, Wu W and Liu J (2023), The evolution characteristics of diamondoids in coal measures and their potential application in maturity evaluation.
Front. Earth Sci. 10:1031799.
doi: 10.3389/feart.2022.1031799

COPYRIGHT
© 2023 Zhai, Cao, Fang, Yuan, Wu and Liu. This is an open-access article distributed under the terms of the Creative Commons Attribution License (CC BY). The use, distribution or reproduction in other forums is permitted, provided the original author(s) and the copyright owner(s) are credited and that the original publication in this journal is cited, in accordance with accepted academic practice. No use, distribution or reproduction is permitted which does not comply with these terms.

The evolution characteristics of diamondoids in coal measures and their potential application in maturity evaluation

Jia Zhai[1,2], Zhenglin Cao[2], Chenchen Fang[2]*, Yilin Yuan[2], Wei Wu[3] and Jinzhong Liu[4]

[1]China University of Mining & Technology, Beijing, China, [2]PetroChina Research Institute of Petroleum Exploration and Development, Beijing, China, [3]Shale Gas Research Institute, Petro China Southwest Oil & Gasfield Company, Chengdu, Sichuan, China, [4]State Key Laboratory of Organic Geochemistry (SKLOG), Guangzhou Institute of Geochemistry, Chinese Academy of Sciences, Guangzhou, China

In this study, gold tube thermal simulation experiments were carried out on the soluble components (extracts) and insoluble components (extracted coal-measure mudstones) of coal-measure mudstones, and diamondoid compounds in the pyrolysis products were quantitatively analyzed. The results showed that diamondoid compounds in the extracts and the extracted coal-measure mudstones had undergone the process of formation and decomposition during thermal evolution. Based on the quantitative composition of the extracts and the extracted coal-measure mudstones, the calculated evolution characteristics of the diamondoid compounds in the coal-measure mudstones were mainly consistent with the results of thermal simulation experiments, indicating that the formation of diamondoid compounds was primarily controlled by the original material source. Some diamondoid maturity parameters (MAI, EAI, TMAI-1) in coal-measure mudstones were consistent with the parameters of the evolution characteristics in marine shale. Therefore, the relationship between these parameters and vitrinite reflectance can be established, to calculate the maturity of marine source rocks. In addition, the evolution characteristics and some diamondoid maturity parameters in the extracts and the extracted coal- measure mudstones showed a good linear relationship, but the specific characteristics were different, which may enable the identification of kerogen cracking and secondary cracking of crude oil.

KEYWORDS

diamondoids, pyrolysis simulation experiment, coal measures, diamondoid parameters, thermal maturity

1 Introduction

Diamondoids, named with reference to their diamond-like structure, are highly resistant to thermal degradation and biodegradation. Thus, they are preserved and enriched during the long and complex geological process, and carry geological information. Therefore, diamondoids have wide applications in petroleum geochemistry, such as oil maturity ascertain (Chen et al., 1996; Li et al., 2000; Zhang et al., 2005; Jiang et al., 2019), oil cracking extent assessment (Dahl et al., 1999), lithofacies discern (Schulz et al., 2001; Chai et al., 2020), secondary change assessment (Jiang et al., 2020), thermochemical sulfate reduction research (Wei et al., 2011), oil spill source identification in accident (Stout and Douglas, 2004; Wang et al., 2006), and so on.

Owing to their presence in immature and sub-mature peat and sedimentary rocks and absence in modern sediments, diamondoids are inferred to be formed in the early diagenesis stage and to be non-biogenic (Schultz et al., 2001; Wei et al., 2006a; Wei et al., 2006b; Wei et al., 2007). According to previous research, there are two main mechanisms for lower diamondoid formation. First, lower diamondoids (adamantanes and diamantanes) are created through Lewis acid-catalyzed rearrangements of polycyclic hydrocarbons (Petrov et al., 1974; Wingert, 1992; Lin and Wilk, 1995). Second, simulation experiments have shown that diamondoids can be produced from high molecular-mass fractions (Giruts et al., 2006; Giruts and Gordadze, 2007), such as kerogen (Wei et al., 2006b), source rocks (Wei et al., 2007b; Fang et al., 2015a; Fang et al., 2015b), crude oils (Fang et al., 2012) and their different group components (Giruts et al., 2006; Giruts and Gordadze, 2007; Fang et al., 2013), and light hydrocarbon component (Fang et al., 2016), C_{16}, C_{19}, C_{22}, C_{34}, C_{36} n-alkanes (Gordadze and Giruts, 2008) and b-ionone (Berwick et al., 2011).

By means of simulation experiments (Fang et al., 2015a), diamondoids can be generated in coal-measure mudstones. However, little work has been done to determine the yield and distribution of diamondoids in coal measure mudstone extracts and extracted mudstones during pyrolysis under non catalytic conditions and their possible interactions. Therefore, in this work, we aimed to investigate these questionsto broaden the potential applications of diamondoids.

2 Materials and methods

2.1 Samples

Coal-measures, are mainly composed of coal, black mudstone and carbonaceous shales (Gong et al., 2018). A sample of coal- measure mudstones from the Xujiahe Formation, Sichuan Basin (used in Fang et al., 2015a), was used in this work, with TOC value of 13.3% and vitrinite reflectance (Ro) of 0.96%. The sample was first ground to pass through 100 mesh and then extracted using the Soxhlet method with a mixed solvent of dichloromethane (DCM) and methanol (MeOH) at a volume ratio of 93:7 for 72 h. The extracts were gently evaporated using a rotary evaporator and dried to a constant weight. The soluble components of the extracts are referred to as mudstone extracts, while the insoluble components, which were further dried in a fume hood, are referred to as extracted coal-measure mudstones in this work. The concentrations of the final extracts and extracted coal-measure mudstones were 6.18 mg/g and 993.82 mg/g in the coal-measure mudstones, respectively.

Gas chromatography–triple quadrupole mass spectrometry (GC–MS–MS) was used to determine the diamondoid concentration (178.77 μg/g) in the mudstone extracts, which was comprised of 155.89 μg/g adamantanes and 22.88 μg/g diamantanes. The target compounds are displayed in Table 1, and in this paper, diamondoids refers to adamantanes and diamantanes combined.

2.2 Simulation experiments

Closed-system pyrolysis experiments were conducted in gold tubes under high-temperature and high-pressure conditions. The detailed pyrolysis method was described previously by Xiong et al. (2004). In the experiments discussed in this work, one end of the gold tubes was sealed by welding, while samples (25–90 mg of extracted mudstone samples or 5–40 mg of extracts) were loaded into the tubes from the other end. The loaded tubes were flushed slowly with argon until the air was completely removed. The other ends of the tubes were then sealed under argon. The sealed gold tubes were mounted in a series of stainless steel autoclaves. Two heating rates (2°C/h and 20°C/h) were used in these autoclaves for the pyrolysis experiments. Between 336 and 600°C, twelve different temperature points were set. At each temperature point, one autoclave was taken out of the oven to air-cool. The gold tubes were then taken out of the cooled autoclave for analysis.

2.3 Quantification of diamondoids

The gold tubes were cleaned with DCM and placed in liquid nitrogen to cool for about 25 min. The tubes were then rapidly cut in half and immersed in a 4 ml sample vial filled with isooctane. A certain amount of isooctane, with n-dodecane-d_{26} as internal standard, was spiked into each vial. To improve the dissolution of pyrolysates, the vials were ultrasonically treated for 10min, and then allowed to stand for 12 h to precipitate the ashphaltenes. An aliquot of the supernatant was placed in a 2 ml vial for the GC-MS-MS analysis of diamondoids. The quantification method was as described by Liang et al. (2012).

TABLE 1 Diamondoids (adamantanes and diamantanes) identified in this work.

Category	Number	Assignment	Abbreviation
Adamantanes	1	Adamantane	A
	2	1-Methyladamantane	1-MA
	3	1,3-Dimethyladamantane	1,3-DMA
	4	1,3,5-Trimethyladamantane	1,3,5-TMA
	5	1,3,5,7-Tetramethyladamantane	1,3,5,7-TeMA
	6	2-Methyladamantane	2-MA
	7	1,4-Dimethyladamantane(*cis*)	1,4-DMA(*cis*)
	8	1,4-Dimethyladamantane(*trans*)	1,4-D MA(*trans*)
	9	1,3,6-Trimethyladamantane	1,3,6-TMA
	10	1,2-Dimethyladamantane	1,2-DMA
	11	1,3,4-Trimethyladamantane(*cis*)	1,3,4-TMA(*cis*)
	12	1,3,4-Trimethyladamantane(*trans*)	1,3,4-TMA(*trans*)
	13	1,2,5,7-Tetramethyladamantane	1,2,5,7-TeMA
	14	1-Ethyladamantane	1-EA
	15	2,6-+2,4-Dimethyladamantane	2,6-+2,4-DMA
	16	1-Ethyl-3-methyladamantane	1-E-3-MA
	17	1,2,3-Trimethyladamantane	1,2,3-TMA
	18	1-Ethyl-3,5-dimethyladamantane	1-E-3,5-DMA
	19	2-Ethyladamantane	2-EA
	20	1,3,5,6-Tetramethyladamantane	1,3,5,6-TeMA
	21	1,2,3,5-Tetramethyladamantane	1,2,3,5-TeMA
	22	1-Ethyl-3,5,7-trimethyladamantane	1-E-3,5,7-TMA
Diamantanes	23	Diamantane	D
	24	4-Methyldiamantane	4-MD
	25	4,9-Dimethyldiamantane	4,9-DMD
	26	1-Methyldiamantane	1-MD
	27	1,4-+2,4-Dimethyldiamantane	1,4-+2,4-DMD
	28	4,8-Dimethyldiamantane	4,8-DMD
	29	1,4,9-Trimethyldiamantane	1,4,9-TMD
	30	3-Methyldiamantane	3-MD
	31	3,4-Dimethyldiamantane	3,4-DMD
	32	3,4,9-Trimethyldiamantane	3,4,9-TMD

3 Results and discussion

3.1 Yields of diamondoids

To apply the results of the simulation experiments carried out under high temperature and fast reaction conditions to explain the actual geological phenomena under low temperature and slow reaction conditions, and to compare them with results obtained in the lab, we used equivalent Ro (EasyRo) (Sweeney and Burnham, 1990) to characterize the thermal maturation (temperature) in the simulation experiments (Figure 1).

In this study, the total contents of 32 diamondoids (22 adamantanes and 10 diamantanes, Table 1) in the pyrolysates were quantitatively analyzed, and the diamondoid yields were used to indicate the changes in the quantities of diamondoids generated during the pyrolysis simulation experiments. The yield of gold tube i, Y_i (μg/g), was defined as the mass of diamondoids in the gold tube, M_i (μg), divided by the mass of sample (extracts or extracted mudstones) in the corresponding gold tube before the pyrolysis simulation experiment, M_0 (g), namely Y_i (μg/g) = M_i (μg)/M_0 (g). Figure 2 shows that the yields of adamantanes and diamantanes, and the total (adamantanes and diamantanes) yield, increased at first, during the slow and rapid generation stages, and then, after peaking, decreased during the destruction stage.

As shown in Figure 2A, during the pyrolysis of the extracts, the yield of diamondoids was 178.36 μg/g (162.86 μg/g of adamantanes and 15.50 μg/g of diamantanes) at the initial

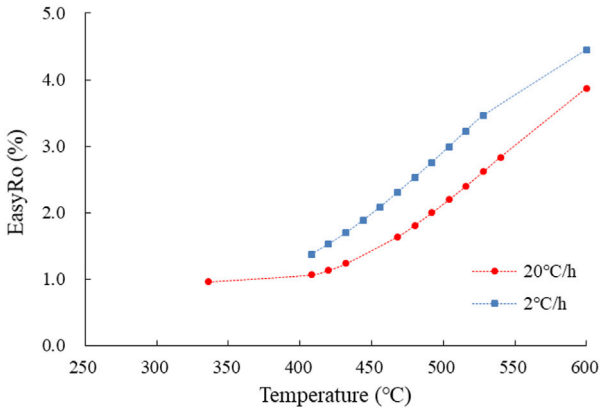

FIGURE 1
Relationship between pyrolysis temperature (°C) and equivalent vitrinite reflectance (EasyRo, %).

point (EasyRo = 0.96%), and reacheed 199.00 μg/g (178.54 μg/g of adamantanes and 20.47 μg/g of diamantanes) at EasyRo 1.14%, indicating that diamondoids were generated slowly below EasyRo 1.14%, in a slow generation stage. With the increase in thermal maturity, the yield increased until it reached a peak value of 303.01 μg/g (270.73 μg/g of adamantanes and 32.27 μg/g of diamantanes) at EasyRo 1.38%, indicating that diamondoids were generated rapidly between EasyRo 1.14% and 1.38%, in a rapid generation stage. The yield then gradually decreased in a fluctuating way to EasyRo 3.23% when the diamondoids were almost all destroyed, in a destruction stage between EasyRo 1.38% and 3.23%. During the pyrolysis process, adamantanes were the major components and had the same evolutionary trend as the diamondoids. The diamantanes were the minor contributors and evolvd more slowly slower than the adamantanes, i.e., the yield of diamantanes reaches a peak value of 45.16 μg/g at EasyRo 2.30%.

During the pyrolysis experiments of the extracted mudstones (Figure 2B), the yield of diamondoids increased slowly from 0.17 μg/g (0.16 μg/g of adamantanes and 0.01 μg/g of diamantanes) at the initial stage (EasyRo 0.96%) to 0.28 μg/g (0.26 μg/g of adamantanes and 0.02 μg/g of diamantanes) at EasyRo 1.07%. After this slow generation stage, the yield of diamondoids began to increase rapidly until EasyRo = 1.38% with a yield of 1.94 μg/g (1.72 μg/g of adamantanes and 0.22 μg/g of diamantanes). Then, the diamondoids entered the destruction stage until almost all were destroyed at EasyRo 2.52%. The adamantanes provided the major contribution to the overall yield. The yield of diamantanes reached a maximum of 0.28 μg/g at EasyRo 1.70%, which was later than the peak of adamantane production.

As shown in Figure 2, the overall evolutionary trends in diamondoid production during extract and extracted mudstone pyrolysis displayed the similar characteristics, which were similar to those for adamantanes, as the main contributors to total diamondoids. However, the trends for diamantanes did not display these similar characteristics.

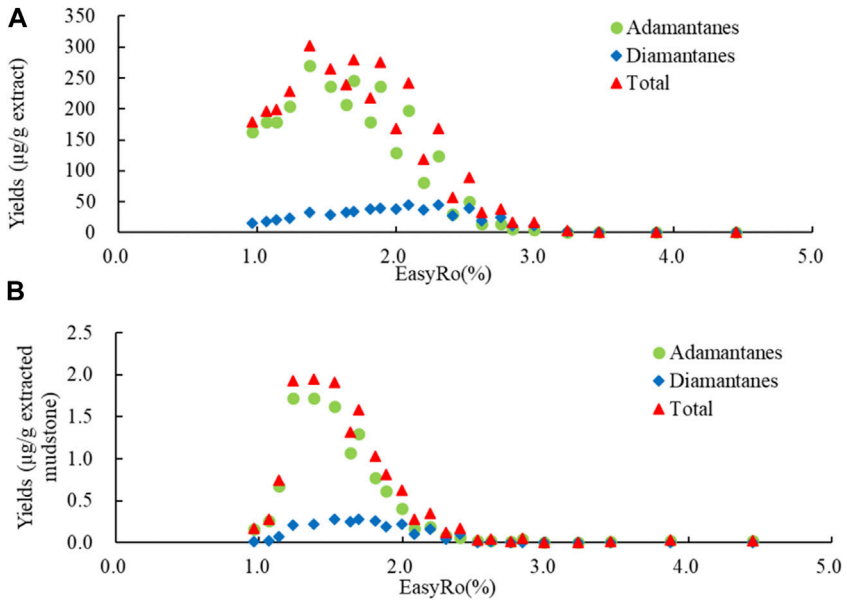

FIGURE 2
Variation in the diamondoid yields (μg/g) with EasyRo (%) during **(A)** extracts and **(B)** extracted mudstones pyrolysis. Total represents all adamantanes and diamantanes in Table 1.

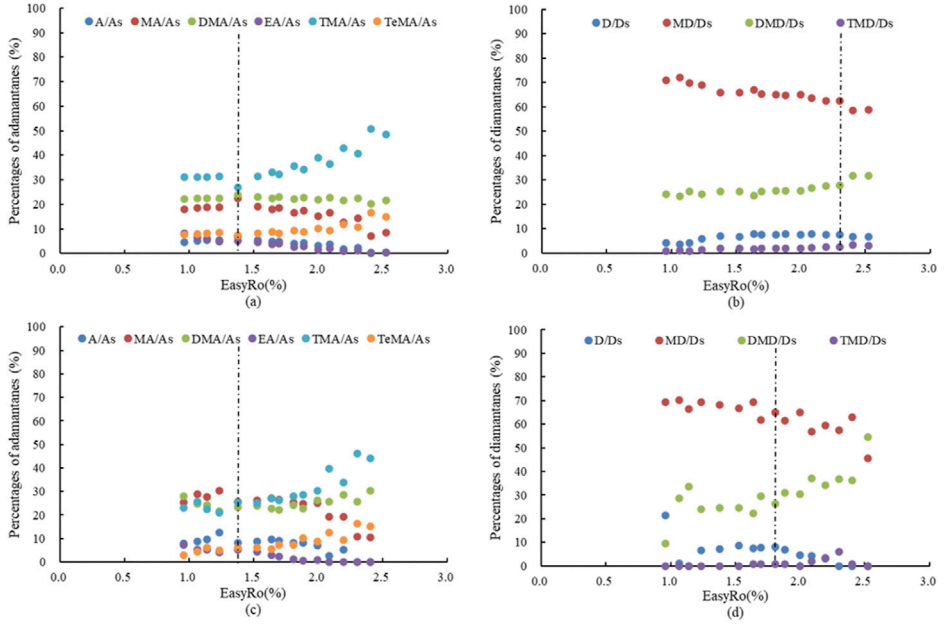

FIGURE 3
The percentage variation of the different alkyl-substituted adamantanes **(A,C)** and diamantanes **(B,D)** of the total adamantanes and diamantanes with extract **(A,B)** and extracted mudstone pyrolysis **(C,D)**, respectively. (A, adamantane; MA, all methyladamantanes; DMA, all dimethyladamantanes; EA,all ethyladamantanes; TMA,all trimethyladamantanes; TeMA, all tetramethyladamantanes; As, all adamantanes; D, diamantine; MD, all methyldiamantanes; DMD, all dimethyldiamantanes; TMD, all trimethyldiamantanes).

Although the diamantanes experienced generation and destruction during both extract and extracted mudstone pyrolysis, the diamantine yield reached a maximum during the extract pyrolysis, which was later than during the extracted mudstone pyrolysis. These results indicated that the mechanism of diamantane formation may be different to that of adamantanes, and the precursor is probably the main controlling factor for diamantane formation. In addition, the maturity of diamantanes corresponding to the maximum yield was higher than that of adamantanes, indicating that the sources or the generation mechanisms of diamantanes differed from those of adamantanes, and the thermal stability of diamantanes higher than that of adamantanes.

3.2 Compositions of diamondoids

To better understand the differences between the extract pyrolysates and the extracted mudstone pyrolysates, the percentage values for the yields of different alkyl-substituted adamantanes and diamantanes generated from extract pyrolysis (Figures 3A,B) and extracted mudstone pyrolysis (Figures 3C,D) were calculated.

During the extract pyrolysis, at the initial point (EasyRo 0.96%), the percentage values for the yields of the different alkyl-substituted adamantanes within the total adamantanes [adamantanes/adamantanes (A/As), methyladamantanes/adamantanes (MA/As), dimethyladamantanes/adamantanes (DMA/As), ethyladamantanes/adamantanes (EA/As), trimethyladamantanes/adamantanes (TMA/As), and tetramethyladamantanes/adamantanes (TeMA/As)] were 4.44%, 17.89%, 22.32%, 8.14%, 31.10%, 7.67%, respectively. These generally remained stable until EasyRo 1.38%, namely, the generation stage, including the slow generation and rapid generation stage, indicating that these compounds (A, MA, DMA, EA, TMA, TeMA) had similar generation rates and formation mechanisms. At this stage, the dominant adamantane compounds were TMA, followed by DMA and MA, and finally TeMA, A and EA. Above EasyRo 1.38%, at the destruction stage, the percentage values for the yields of different alkyl-substituted adamantanes in the total adamantanes began to change. As shown in Figure 3, the percentage values of TMA/As and TeMA/As increased, while the percentage values of MA/As, EA/As and A/As decrease, and the percentage values of DMA/As generally remained stable. These results indicated that these compounds (A, MA, DMA, EA, TMA, TeMA) had different destruction rates at this stage. The adamantanes with a higher carbon number (such as TMA and TeMA) had slower cracking speeds than the adamantanes with a lower carbon number (such as MA, EA, and A). Although DMA and EA have the same carbon number, their destruction characteristics were different, indicating that the different chemical structures

determined the various pyrolysis properties. In other words, these adamantanes had different destruction mechanisms, and TMA and TeMA were relatively more stable than MA, EA, and A.

The percentage values for the yield of different alkyl-substituted diamantanes within the total diamantanes [diamantine/diamantanes (D/Ds), methyldiamantanes/diamantanes (MD/Ds), dimethyldiamantanes/diamantanes (DMD/Ds), and trimethyldiamantanes/diamantanes (TMD/Ds)] were 4.26%, 70.88%, 24.08%, 0.78% at the initial point (EasyRo 0.96%). They generally changed slowly, almost constantly, at the generation stage (EasyRo 0.96%–2.30%), including the slow generation stage and rapid generation stage, indicating that these compounds (D, MD, DMD, TMD) had similar generation rates and formation mechanisms. At this stage, the dominant diamantane compounds were MD, followed by DMD, and finally D and TMD. At the destruction stage, the percentage values began to change rapidly, with DMD/Ds and TMD/Ds increasing and D/Ds and MD/Ds decreasing, indicating that these compounds (D, MD, DMD, TMD) had different destruction rates at this stage. The diamantanes with a higher carbon number (such as DMD and TMD) had slower cracking speed than the diamantanes with a lower carbon number (such as D and MD). In summary, these diamantanes had different cracking mechanisms, and DMD and TMD were relatively more stable than D and MD.

During the extracted mudstone pyrolysis, the percentage values for the yield of different alkyl-substituted adamantanes within the total adamantanes (A/As, MA/As, DMA/As, EA/As, TMA/As, TeMA/As) were 7.98%, 25.45%, 27.88%, 7.36%, 23.09%, 2.88%, respectively, at EasyRo 0.96%. Their fluctuations were very small at the generation stage (EasyRo 0.96%–1.38%), with the dominant adamantane compounds being DMA, MA, and TMA, followed by TeMA, A and EA. At the destruction stage (EasyRo > 1.38%), the percentage values of TMA/As and TeMA/As increased, and the percentage values of MA/As, A/As and EA/As decreased, while the DMA/As values showed small fluctuations within a certain range, indicating faster cracking speeds for A, MA, and EA than TMA and TeMA, and greater relative stability of TMA and TeMA than MA, EA, and A. Similar to the results obtained during the extract pyrolysis, these findings indicated that these adamantanes (A, MA, DMA, EA, TMA, TeMA) had similar generation rates and formation mechanism at the generation stage, but different destruction rates and destruction mechanisms at the destruction stage.

For diamantanes, the percentage values for the yields of different alkyl-substituted diamantanes within the total diamantanes (D/Ds, MD/Ds, DMD/Ds, TMD/Ds) generally showed small changes at the generation stage (lower than EasyRo 1.70%). Then, at the destruction stage, the changes became somewhat larger, with DMD/Ds and TMD/Ds increasing, and MD/Ds and D/Ds decreasing. Similar to the results obtained during the extract pyrolysis, these findings indicated that these adamantanes (D, MD, DMD, TMD) had similar generation rates and formation mechanisms at the generation stage, and different destruction rates and destrution mechanisms at the destruction stage.

Comparing the evolutionary characteristics between the extract pyrolysis and the extracted mudstone pyrolysis, as shown in Figure 3, there was no significant change in the percentage values for either adamantanes or diamantanes at the generation stage. Hence, differences at the initial point may be decided by the precursors in the organic matter. As, there was no significant difference among the different alkyl-substituted compounds, at the destruction stage, the evolutionary characteristics may therefore be decided by the pyrolysis. Moreover, the higher the carbon number, the better the thermal stability, as in TMA/As, TeMA/As, DMD/Ds, and TMD/Ds with increasing EasyRo caused by the high thermal stability and low cracking rate of TMA, TeMA, DMD, and TMD.

3.3 Possible interaction between extracts and extracted mudstones

In the study by Fang et al. (2015a), the generation and evolution of diamondoids in coal measures was discussed. In addition, previous studies have shown that the extract along with kerogen from marine source rocks, can produce diamondoids during the maturing process (Fang et al., 2015b). To properly understand the source and origin of diamondoids in coal measures, pyrolysis experiments were undertaken on both the extracts and extracted mudstones. It is also valuable to determine whether there is a mutual effect between the soluble and insoluble components of coal-measure mudstones.

We calculated the yields of diamondoids during the mudstone pyrolysis, extract pyrolysis and extracted mudstone pyrolysis, as well as the contents of extracts and extracted mudstones within the source rock, to obtain the yields of calculated diamondoids (extracts and extracted mudstones) (Figure 4). We then compared the yields of measured diamondoids during the mudstone pyrolysis (Fang et al., 2015a) to obtained the measured diamondoids, as shown in Figure 4. In general, the diamondoids were shown to undergo generation and destruction during the coal mudstone pyrolysis.

The calculated diamondoids (extracts and extracted mudstones) reached a maximum value, 3.80 μg/g coal measures, at EasyRo 1.38% as shown in Figure 4, while the calculated diamondoids reached a maximum value, 3.66 μg/g coal measures, at EasyRo 1.53% (Fang et al., 2015a). Both the calculated and measured diamondoids during the mudstone pyrolysis reached similar maximum yields of diamondoids, and also their levels of maturity similarly corresponded to the maximum yields of diamondoids. These results, therefore, indicated that the main controlling factor of yield was the

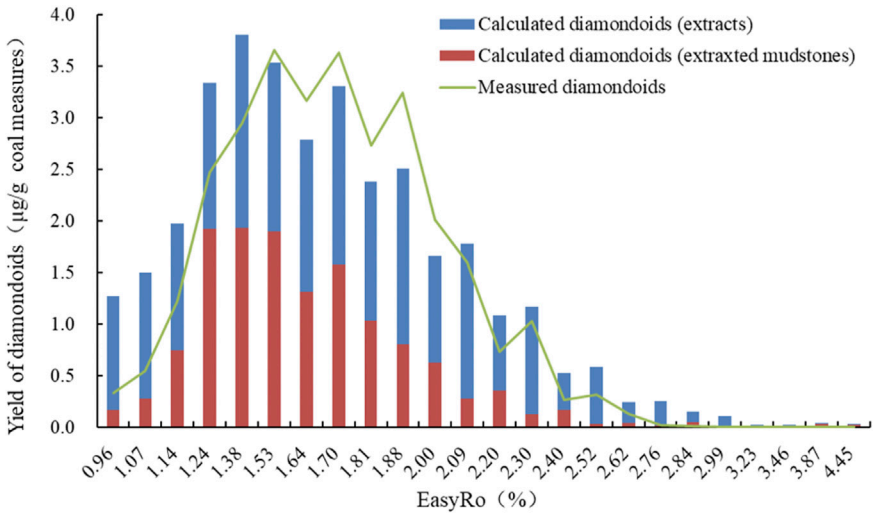

FIGURE 4
Variation in the yields (μg/g) of calculated diamondoids (extracts), calculated diamondoids (extracted mudstones), and measured diamondoids (Fang et al., 2015a) with EasyRo (%).

source matter and not the interaction between the extracts and extracted mudstones.

The overall calculated evolutionary trend of diamondoids was consistent with the measurements of the calculated yields (Fang et al., 2015a). There were no obvious interactions or mutual effects between the soluble and insoluble components. However, at the low yield stages (EasyRo ≤ 1.14% and EasyRo ≥ 2.40%), there was a big difference between the measured and calculated yields, as shown in Figure 4, probably caused by measurement error when the yield was very low. Moreover, the inhibitory effect of the minerals in the coal-measure mudstones on the generation of diamondoids (Wei et al., 2006c) was another possible reason, but this requires further analysis.

The major contributors to the diamondoid generation were the extracts (Figure 4), which accounted for 42.3%–96.1% of the overall yield. At the initial thermal evolution (EasyRo 0.96%), 86.8% of the generated diamondoids were attributed to the extracts. However, with the increase in maturity, the contribution from the extracts gradually decreased and the minimum yield was 42.3% at EasyRo 1.24%. In the subsequent destruction stage, the contribution from the extracts increased again until it reached a maximum of 96.1% at EasyRo 2.99%. Meanwhile, the contribution from the extracted coal mudstones, displayed the opposite evolutionary trend, with the contribution varying from 3.9 to 57.7%. This indicated that, at the generation stage, the overall generation rate of diamondoid compounds in the extracted coal-measure mudstones was faster than that in the soluble organic matter, which may be related to the source of the parent material. This was consistent with the results from research on marine shale, which indicated that the major source of diamondoids in marine shales is the soluble extracts, with a ratio of 59.7%–100% (Fang et al., 2015b).

In summary, the major source of diamondoids was the extracts, which accounted for 42.6%–96.1% of the total yield. The rest was contributed by the extracted mudstones and there were no obvious mutual effects of the soluble and insoluble components on each other. Both the adamantanes and diamantanes had the same major source as the overall diamondoids. The changes in contributions of the extracts, along with the insoluble components, shared the same trends for the adamantanes and diamantanes.

3.4 Diamondoid parameters

A lot of work has been carried out on diamondoid maturity parameters (Chen et al., 1996; Grice et al., 2000; Schulz et al., 2001; Zhang et al., 2005; Wei et al., 2007b), including methyladamantane index [MAI, 1-MA/(1-MA+2-MA)], dimethyladamantane index-1 [DMAI-1,1,3-DMA/(1,2-DMA+1,3-DMA)], dimethyladamantane index-2 [DMAI-2, 1,3-DMA/(1,3-DMA+1,4-DMA)], ethyladamantane index [EAI, 1-EA/(1-EA+2-EA)], trimethyladamantane index-1 [TMAI-1, 1,3,5-TMA/(1,3,5-TMA+1,3,4-TMA)], trimethyladamantane index-2 [TMAI-2, 1,3,5-TMA/(1,3,5-TMA+1,3,6-TMA)], methyldiamantane index [MDI, 4-MD/(4-MD+1-MD+3-MD)], dimethyldiamantane index-1 [DMDI-1,

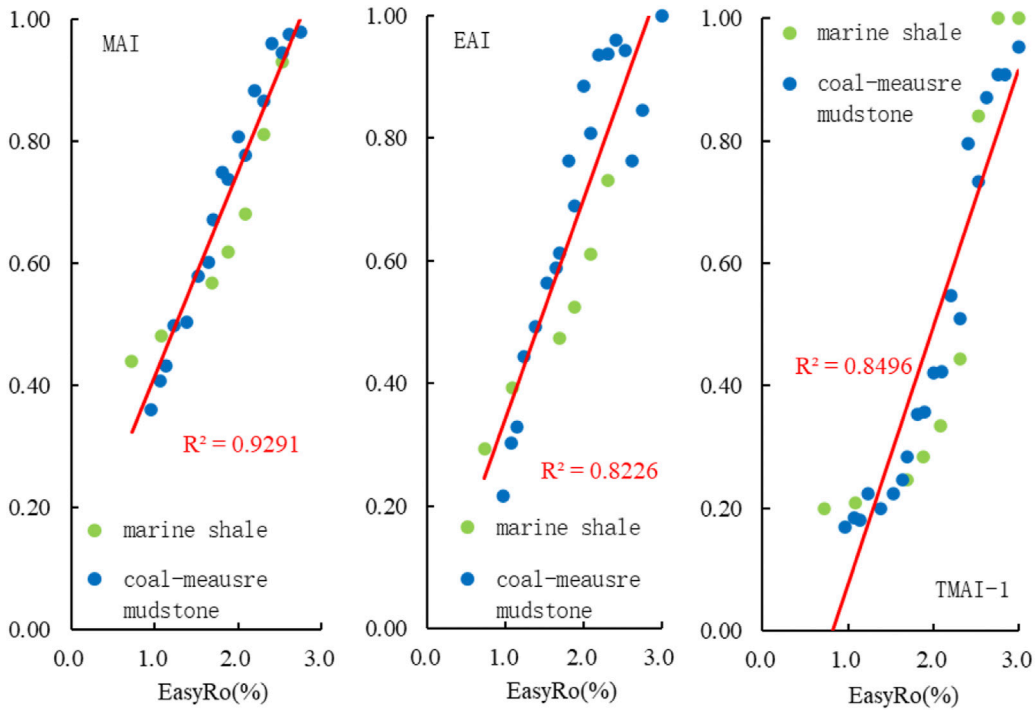

FIGURE 5
Change diagram of diamondoid parameters (MAI, EAI, TMAI-1) during marine shale (Fang et al., 2015b) and coal-measure mudstone pyrolysis.

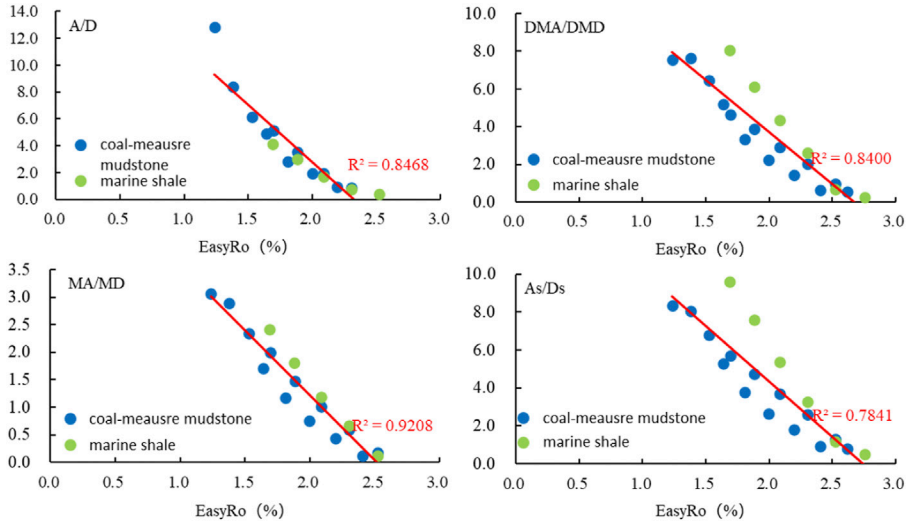

FIGURE 6
Change diagram of diamondoid yield ratios (A/D, MA/MD, DMA/DMD, As/Ds) during marine shale (Fang et al., 2015b) and coal-measure mudstone pyrolysis.

4,9-DMD/(4,9-DMD+3,4-DMD)], and dimethyldiamantane index-2 [DMDI-2, 4,9-DMD/(4,9-DMD+4,8-DMD)].

As pointed out in Figure 5, MAI, EAI, and TMAI-1 are well correlated with maturity (EasyRo, %) in the evolution of coal-measure mudstones. Comparing these parameters (MAI, EAI, and TMAI-1) during marine source rock pyrolysis (Fang et al., 2015b), MAI, EAI, and TMAI-1 were found to have the same evolutionary trend, with increasing EasyRo (%), between marine source rock pyrolysis (Fang et al., 2015b) and coal-measure mudstone pyrolysis. In other words, the source of organic matter had no significant effect on the maturity parameters of diamondoid compounds during the pyrolysis of source rocks, and the evolutionary characteristics of diamondoid maturity parameters in different types of source rocks are very similar, within the EasyRo range of 1.0–3.0%, with the correlation coefficients ranging from 0.8226 to 0.9291.

It is also pointed out in Figure 6 that there was a strong correlation between thermal maturity and the following yield (concentration) ratios: A/D, MA/MD, DMA/DMD and As/Ds (adamantanes/diamantanes) within certain EasyRo ranges. Comparing with these parameters (A/D, MA/MD, DMA/DMD and As/Ds) during the marine source rock pyrolysis (Fang et al., 2015b), we also found that A/D, MA/MD, DMA/DMD and As/Ds have the same evolution trend with EasyRo (%) increasing between marine source rock pyrolysis (Fang et al., 2015b) and coal-measure mudstone pyrolysis, within the EasyRo range of 1.2%–2.5%, with correlation coefficients ranging from 0.7841 to 0.9208.

In summary, both the isomerization indices (MAI, EAI and TMAI-1) and the yield indices (A/D, MA/MD, DMA/DMD and As/Ds) during coal-measure mudstone pyrolysis were shown to have strong correlations with thermal maturity. Similar correlations were also found in highly cracked marine shales (Fang et al., 2015b). This indicated that these parameters were not dependent on the source of organic matter. Therefore, it is possible that the isomerization and yield indices can be more broadly applied for maturity assessment in different samples.

3.4.1 Maturity evaluation of marine source rocks

The maturity of coal-measure source rocks can be measured by the Ro, as a commonly used maturity measure. Whereas due to the lack of vitrinite in marine source rocks, the maturity evaluation of source rocks and crude oil has always been difficult.

Oil and gas exploration in the Tarim and Ordos basins has confirmed the important role of lower Paleozoic marine sedimentary source rocks in China. There are two notable characteristics of the lower Paleozoic marine sediments: high maturity (generally high- and over-mature stages, Ro in the range 1.0%–2.0%) and little organic matter. Thus, assessing the maturity of these lower Paleozoic hydrocarbon source rocks is difficult. There may be two reasons for this. First, vitrinite reflectance cannot be detected to assess maturity, for vitrinite derived from higher plants is absent in marine sediments. Second, conventional molecular organic geochemical maturity parameters, such as biomarker parameters (Song et al., 2016; Song et al., 2017; Xu et al., 2021; Xu et al., 2022, etc), may be invalid at the high- to over-mature stage.

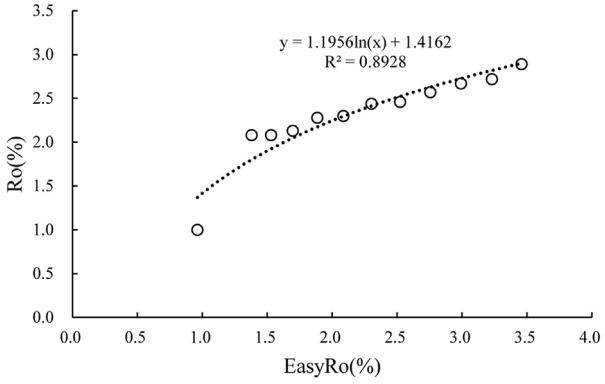

FIGURE 7
Relationship between vitrinite reflectance (Ro) and equivalent vitrinite reflectance (EasyRo).

There is abundant vitrinite in coal-measure mudstones, and maturity can be characterized by measuring Ro. From the relationship between the diamondoid indics and maturity values seen in Figures 5, 6, the relationship between Ro and EasyRo can be established by using the measurement of Ro in coal-measure mudstones, as shown in Figure 7. Therefore, the diamondoid parameters can be used to calculate the maturity parameter Ro, so as to further expand the scope for application of the diamondoid maturity parameter and the comparability of the obtained maturity value.

3.4.2 Kerogen cracking and crude oil secondary cracking

During the separate pyrolysis of the soluble and insoluble organic matter components in the coal-measure mudstones, the evolutionary characteristics of yield were similar, but there were certain differences in the diamondoid parameters. Under the same maturity conditions, the diamondoid parameters (MAI, EAI, TAI-1) in the thermal evolution of the extracts were lower than the diamondoid parameters in the evolution of the extracted coal-measure mudstones (Figure 8). Therefore, it can be assumed that early hydrocarbon expulsion causes the difference in the diamondoid parameters of the reservoir and source rock, and is the reason why the diamondoid parameters from crude oil secondary cracking are lower than those from kerogen cracking.

This indicates that, the evolutionary characteristics of total diamondoid yields in soluble and insoluble organic matter may be different, but the main controlling factor is the original organic matter. Meanwhile, the difference in the original

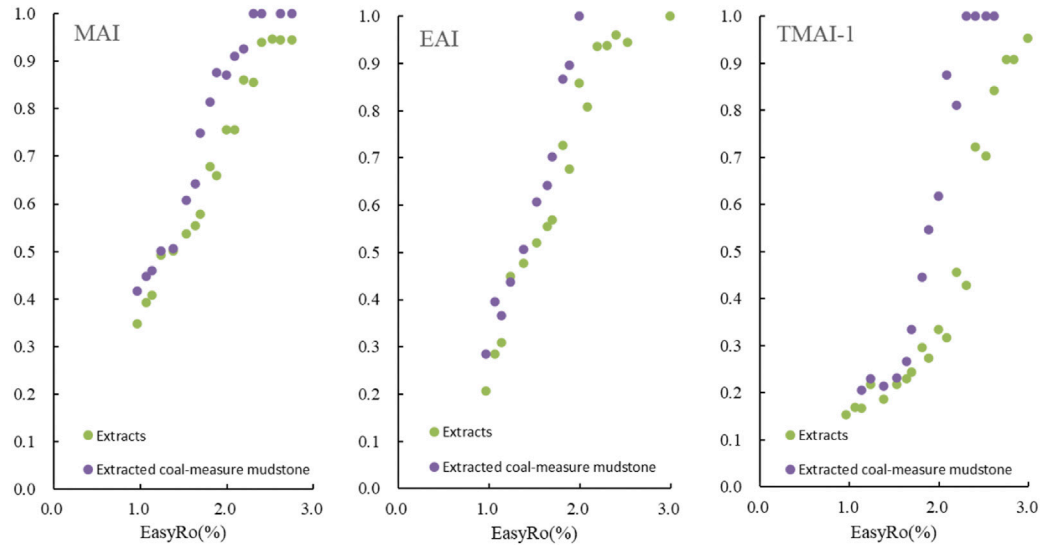

FIGURE 8
Change diagram of diamondoid parameters (MAI, EAI, TMAI-1) during extract and extracted coal-measure mudstone pyrolysis.

organic matter may also lead to the differences in diamondoid parameters, which may distinguish kerogen cracking and crude oil secondary cracking.

Therefore, the diamondoid parameters (MAI, EAI, TAI-1) in late hydrocarbon expulsion may be similar to those of the source rocks, while the diamondoid parameters formed by geological processes after hydrocarbon expulsion in the early stage may be different from those of the source rocks.

4 Summary

(1) We conducted pyrolysis simulation experiments on both the extracts and the extracted mudstones from coal-measure mudstones and quantified the amount of diamondoids in the pyrolysates. The results showed that both the extracts and the extracted mudstones generated diamondoids and that both experienced two-stage pyrolysis (generation and destruction).

(2) Based on the measured diamondoid yields in the extracts and the extracted mudstones along with the composition of the coal-measure mudstone samples (the percentage of the extracts and the extracted mudstones), the results showed that the extracts formed the majority of the total diamondoid yield (42.3%–96.1%). In addition, by comparing the calculated and measured yields, the diamondoid yields depend on the original matter source. This indicated that there was no obvious mutual effects of the extracts and the extracted mudstones on each other in terms of diamondoid generation.

(3) In the comparison of the diamondoid parameters during pyrolysis between coal-measure mudstones and marine shales, it was found that some parameters (MAI, EAI, and TAMI-1), had a strong linear relationship with maturity within the range of EasyRo 1.0%–3.0% and correlation coefficients of 0.8226–0.9291. Another example was taken from the yield ratios including A/D, MA/MD, DMA/DMD as well as As/Ds. These yield ratios were strongly correlated with maturity within the EasyRo 1.2%–2.5% range and the correlation coefficients varied from 0.7841 to 0.9208. All of the strong correlations mentioned above suggested that these parameters can be widely used as proxies for maturity in broader geological conditions.

(4) Through the measurement of Ro in coal-measure mudstones, the diamondoid parameters could be converted directly into Ro, which is convenient for comparison with maturity in other studies. In addition, the difference in diamondoid parameters between the extracts and extracted kerogen could reflect the difference between kerogen cracking and crude oil secondary cracking.

Data availability statement

The raw data supporting the conclusion of this article will be made available by the authors, without undue reservation.

Author contributions

JZ: data curation, writing—original draft preparation, validation. ZC: investigation, supervision. CF: conceptualization, writing-

reviewing and editing, validation. YY: methodology, data curation. WW: investigation, formal analysis. JL: methodology.

Funding

This work was financially supported by the National Natural Science Foundation of China (Grant Nos. 42172184 and 41503044), and the Scientific Research and Technological Development Project of China National Petroleum Corporation (Grant No. 2021DJ0601).

Acknowledgments

We are grateful to Zhang W. B. for his assistance with the GC-MS-MS analysis, and Xu A., Li Y., and Yang X. for their help with the pyrolysis experiments.

Conflict of interest

The authors JZ, ZC, CF and YY were employed by PetroChina Research Institute of Petroleum Exploration and Development. The author WW was employed by PetroChina Southwest Oil & Gasfield Company.

The remaining authors declare that the research was conducted in the absence of any commercial or financial relationships that could be construed as a potential conflict of interest.

Publisher's note

All claims expressed in this article are solely those of the authors and do not necessarily represent those of their affiliated organizations, or those of the publisher, the editors and the reviewers. Any product that may be evaluated in this article, or claim that may be made by its manufacturer, is not guaranteed or endorsed by the publisher.

References

Berwick, L., Alexander, R., and Pierce, K. (2011). Formation and reactions of alkyl adamantanes in sediments: Carbon surface reactions. *Org. Geochem.* 42, 752–761. doi:10.1016/j.orggeochem.2011.05.008

Chai, Z., Chen, Z. H., Liu, H., Cao, Z. C., Cheng, B., Wu, Z. P., et al. (2020). Light hydrocarbons and diamondoids of light oils in deep reservoirs of Shuntuoguole Low Uplift, Tarim Basin: Implication for the evaluation on thermal maturity, secondary alteration and source characteristics. *Mar. Pet. Geol.* 117, 104388–388. doi:10.1016/j.marpetgeo.2020.104388

Chen, J. H., Fu, J. M., Sheng, G. Y., Liu, D. H., and Zhang, J. J. (1996). Diamondoid hydrocarbon ratios: Novel maturity indices for highly mature crude oils. *Org. Geochem.* 25, 179–190. doi:10.1016/S0146-6380(96)00125-8

Dahl, J. E., Moldowan, J. M., Peters, K. E., Claypool, G. E., Rooney, M. A., Michael, G. E., et al. (1999). Diamondoid hydrocarbons as indicators of natural oil cracking. *Nature* 399, 54–57. doi:10.1038/19953

Fang, C. C., Wu, W., Liu, D., and Liu, J. Z. (2015a). Evolution characteristics and application of diamondoids in coal measures. *J. Nat. Gas Geoscience* 26 (1), 93–99. doi:10.1016/j.jnggs.2016.02.001

Fang, C. C., Xiong, Y. Q., Li, Y., Chen, Y., and Tang, Y. J. (2015b). Generation and evolution of diamondoids in source rock. *Mar. Pet. Geol.* 67, 197–203. doi:10.1016/j.marpetgeo.2015.05.018

Fang, C. C., Xiong, Y. Q., Li, Y., Liang, Q. Y., Wang, T. S., and Li, Y. X. (2016). The effect of volatile components in oil on evolutionary characteristics of diamondoids during oil thermal pyrolysis. *Sci. China Earth Sci.* 59, 362–370. doi:10.1007/s11430-015-5163-x

Fang, C. C., Xiong, Y. Q., Liang, Q. Y., and Li, Y. (2012). Variation in abundance and distribution of diamondoids during oil cracking. *Org. Geochem.* 47, 1–8. doi:10.1016/j.orggeochem.2012.03.003

Fang, C., Xiong, Y., Li, Y., Chen, Y., Liu, J., Zhang, H., et al. (2013). The origin and evolution of adamantanes and diamantanes in petroleum. *Geochim. Cosmochim. Acta* 120, 109–120. doi:10.1016/j.gca.2013.06.027

Giruts, M. V., and Gordadze, G. N. (2007). Generation of adamantanes and diamantanes by thermal cracking of polar components of crude oils of different genotypes. *Pet. Chem.* 47, 12–22. doi:10.1134/s0965544107010021

Giruts, M. V., Rusinova, G. V., and Gordadze, G. N. (2006). Generation of adamantanes and diamantanes by thermal cracking of high-molecular-mass saturated fractions of crude oils of different genotypes. *Pet. Chem.* 46, 225–236. doi:10.1134/S0965544106040025

Gong, D. Y., Li, J. Z., Ablimit, I., He, W. J., Lu, S., Liu, D. G., et al. (2018). Geochemical characteristics of natural gases related to Late Paleozoic coal measures in China. *Mar. Petroleum Geol.* 96, 474–500. doi:10.1016/j.marpetgeo.2018.06.017

Gordadze, G. N., and Giruts, M. V. (2008). Synthesis of adamantane and diamantane hydrocarbons by high-temperature cracking of higher n-alkanes. *Pet. Chem.* 48, 414–419. doi:10.1134/S0965544108060029

Grice, K., Alexander, R., and Kagi, R. I. (2000). Diamondoid hydrocarbon ratios as indicators of biodegradation in Australian crude oils. *Org. Geochem.* 31, 67–73. doi:10.1016/s0146-6380(99)00137-0

Jiang, W. M., Li, Y., and Xiong, Y. Q. (2020). Reservoir alteration of crude oils in the Junggar Basin, northwest China: Insights from diamondoid indices. *Mar. Pet. Geol.* 119, 104451. doi:10.1016/j.marpetgeo.2020.104451

Jiang, W. M., Li, Y., and Xiong, Y. Q. (2019). Source and thermal maturity of crude oils in the Junggar Basin in northwest China determined from the concentration and distribution of diamondoids. *Org. Geochem.* 128, 148–160. doi:10.1016/j.orggeochem.2019.01.004

Li, J. G., Philp, P., and Cui, M. Z. (2000). Methyl Diamantane index (MDI) as a maturity parameter for Lower Palaeozoic carbonate rocks at high maturity and overmaturity. *Org. Geochem.* 31, 267–272. doi:10.1016/s0146-6380(00)00016-4

Liang, Q. Y., Xiong, Y. Q., Fang, C. C., and Li, Y. (2012). Quantitative analysis of diamondoids in crude oils using gas chromatography-triple quadrupole mass spectrometry. *Org. Geochem.* 43, 83–91. doi:10.1016/j.orggeochem.2011.10.008

Lin, R., and Wilk, Z. A. (1995). Natural occurrence of tetramantane ($C_{22}H_{28}$), pentamantane ($C_{26}H_{32}$) and hexamantane ($C_{30}H_{36}$) in a deep petroleum reservoir. *Fuel* 74, 1512–1521. doi:10.1016/0016-2361(95)00116-m

Petrov, A., Arefjev, D. A., Yakubson, Z. V., Tissot, B., Bienner, F., Schneider, A., et al. (1974). *Advances in organic geochemistry*, 31. Paris: Editions Technip, 1617–1625. doi:10.1021/jo01343a070Hydrocarbons of adamantane series as indices of petroleum catagenesisFormation of perhydrophenalenes and polyalkyladamantanes by isomerization of tricyclic perhydroaromatics*J. Org. Chem.*

Schulz, L. K., Wilhelms, A., Rein, E., and Steen, A. S. (2001). Application of diamondoids to distinguish source rock facies. *Org. Geochem.* 32, 365–375. doi:10.1016/S0146-6380(01)00003-1

Song, D. F., Simoneit, B. R., and He, D. F. (2017). Abundant tetracyclic terpenoids in a Middle Devonian foliated cuticular liptobiolite coal from northwestern China. *Org. Geochem.* 107, 9–20. doi:10.1016/j.orggeochem.2017.02.010

Song, D. F., Wang, T. G., and Li, M. J. (2016). Geochemistry and possible origin of the hydrocarbons from wells Zhongshen1 and Zhongshen1C, tazhong uplift. *Sci. China Earth Sci.* 59, 840–850. doi:10.1007/s11430-015-5226-z

Stout, S. A., and Douglas, G. S. (2004). Diamondoid hydrocarbons – application in the chemical fingerprinting of natural gas condensate and gasoline. *Environ. Forensics* 5, 225–235. doi:10.1080/15275920490886734

Sweeney, J. J., and Burnham, A. K. (1990). Evaluation of a simple-model of vitrinite reflectance based on chemical-kinetics. *Am. Assoc. Pet. Geol. Bull.* 74, 1559–1570. doi:10.1306/0C9B251F-1710-11D7-8645000102C1865D

Wang, Z. D., Yang, C., Hollebone, B., and Fingas, M. (2006). Forensic fingerprinting of diamondoids for correlation and differentiation of spilled oil and petroleum products. *Environ. Sci. Technol.* 40, 5636–5646. doi:10.1021/es060675n

Wei, Z. B., Mankiewicz, P., Walters, C., Qian, K. N., Phan, N. T., Madincea, M. E., et al. (2011). Natural occurrence of higher thiadiamondoids and diamondoidthiols in a deep petroleum reservoir in the Mobile Bay gas field. *Org. Geochem.* 42, 121–133. doi:10.1016/j.orggeochem.2010.12.002

Wei, Z. B., Moldowan, J. M., Dahl, J., Goldstein, T. P., and Jarvie, D. M. (2006a). Diamondoids and molecular biomarkers generated from modern sediments in the absence and presence of minerals during hydrous pyrolysis. *Org. Geochem.* 37, 891–911. doi:10.1016/j.orggeochem.2006.04.008

Wei, Z. B., Moldowan, J. M., Dahl, J., Goldstein, T. P., and Jarvie, D. M. (2006b). The catalytic effects of minerals on the formation of diamondoids from kerogen macromolecules. *Org. Geochem.* 37, 1421–1436. doi:10.1016/j.orggeochem.2006.07.006

Wei, Z. B., Moldowan, J. M., Jarvie, D. M., and Hill, R. (2006c). The fate of diamondoids in coals and sedimentary rocks. *Geol.* 34, 1013–1016. doi:10.1130/G22840A.1

Wei, Z. B., Moldowan, J. M., Peters, K. E., Wang, Y., and Xiang, W. (2007b). The abundance and distribution of diamondoids in biodegraded oils from the San Joaquin Valley: Implications for biodegradation of diamondoids in petroleum reservoirs. *Org. Geochem.* 38, 1910–1926. doi:10.1016/j.orggeochem.2007.07.009

Wei, Z. B., Moldowan, J. M., Zhang, S. C., Hill, R., Jarvie, D. M., Wang, H. T., et al. (2007). Diamondoid hydrocarbons as a molecular proxy for thermal maturity and oil cracking: Geochemical models from hydrous pyrolysis. *Org. Geochem.* 38, 227–249. doi:10.1016/j.orggeochem.2006.09.011

Wingert, W. S. (1992). Gc-ms analysis of diamondoid hydrocarbons in Smackover Petroleums. *Fuel* 71, 37–43. doi:10.1016/0016-2361(92)90190-Y

Xiong, Y. Q., Geng, A. S., and Liu, J. Z. (2004). Kinetic-simulating experiment combined with GC-IRMS analysis: Application to identification and assessment of coal-derived methane from zhongba gas field (Sichuan Basin, China). *Chem. Geol.* 213, 325–338. doi:10.1016/j.chemgeo.2004.07.007

Xu, H. Y., Liu, Q. Y., Zhu, D. Y., Meng, Q. Q., Jin, Z. J., Fu, Q., et al. (2021). Hydrothermal catalytic conversion and metastable equilibrium of organic compounds in the Jinding Zn/Pb ore deposit. *Geochimica Cosmochimica Acta* 307, 133–150. doi:10.1016/j.gca.2021.05.049

Xu, H. Y., Liu, Q. Y., Zhu, D. Y., Peng, W. L., Meng, Q. Q., Wang, J. B., et al. (2022). Molecular evidence reveals the presence of hydrothermal effect on ultra-deep-preserved organic compounds. *Chem. Geol.* 608, 121045. doi:10.1016/j.chemgeo.2022.121045

Zhang, S. C., Huang, H. P., Xiao, Z. Y., and Liang, D. G. (2005). Geochemistry of palaeozoic marine petroleum from the Tarim basin, NW China. Part 2: Maturity assessment. *Org. Geochem.* 36, 1215–1225. doi:10.1016/j.orggeochem.2005.01.014